Discovery and Evaluation of 2-Anilino-5-aryloxazoles as a Novel Class of VEGFR2 Kinase Inhibitors

Philip A. Harris,* Mui Cheung, Robert N. Hunter III, Matthew L. Brown,† James M. Veal,† Robert T. Nolte, Liping Wang, Wendy Liu,† Renae M. Crosby, Jennifer H. Johnson, Andrea H. Epperly, Rakesh Kumar, Deirdre K. Luttrell,† and Jeffrey A. Stafford†

GlaxoSmithKline, Five Moore Drive, Research Triangle Park, North Carolina 27709

Received June 11, 2004

A series of derivatives of 2-anilino-5-phenyloxazole (**5**) has been identified as inhibitors of VEGFR2 kinase. Herein we describe the structure−activity relationship (SAR) of this novel template. Optimization of both aryl rings led to very potent inhibitors at both the enzymatic and cellular levels. Oxazole **39** had excellent solubility and good oral PK when dosed as the bis-mesylate salt and demonstrated moderate in vivo efficacy against HT29 human colon tumor xenografts. X-ray crystallography confirmed the proposed binding mode, and comparison of oxazoles **39** and **46** revealed interesting differences in orientation of 2-pyridyl and 3-pyridyl rings, respectively, attached at the meta position of the 5-phenyl ring.

Introduction

The growth of solid tumors is dependent on the formation of new capillaries from existing blood vessels.[1] This process, known as angiogenesis, is facilitated by a number of mitogenic endogenous proteins, of which vascular endothelial growth factor (VEGF) is thought to be key. VEGF is upregulated by tumors and induces a mitogenic response on binding to the tyrosine kinase receptor VEGFR2 (KDR/Flk-1) on nearby endothelial cells.[2] Inhibition of angiogenesis via blocking of this pathway has attracted widespread interest as an approach to anticancer therapy.[3] The first successful clinical validation to this approach came recently from phase III trials of bevacizumab (Avastin), a monoclonal antibody to VEGF, which when combined with chemotherapy in metastatic colorectal cancer met its primary endpoint of improving survivial.[4] Other large-molecule therapeutic approaches currently in clinical development include neutralizing antibodies to VEGFR2[5] and a soluble VEGF decoy-receptor.[6] A number of orally active small-molecule inhibitors of VEGFR2 are currently undergoing clinical evaluation, including the anilinophthalazine (**1**) (PTK787/Vatalanib, Schering/Novartis, phase III),[7] the anilinoquinazoline (**2**) (ZD6474, AstraZeneca, phase II),[8] the indolinone (**3**) (SU11248/Sutent, Pfizer, phase III),[9] and the isothiazole (**4**) (CP-547,632, Pfizer, phase I/II).[10]

As part of our efforts to develop small molecule inhibitors of the VEGFR2 kinase domain, screening of our sample collection identified 2-anilino-5-phenyloxazole (**5**) as an initial hit.[11] This oxazole was an attractive starting point, exhibiting moderate VEGFR2 enzyme potency (IC_{50} = 1.2 μM) and inhibiting VEGF-induced proliferation of human umbilical vein endothelial cells (HUVEC) with an IC_{50} of 3 μM. As a measure of selectivity, **5** was found to only weakly inhibit the basic fibroblast growth factor (b-FGF) induced proliferation of HUVEC cells (IC_{50} = 24 μM). Herein, we report on the SAR of this series, the enzyme binding mode as evidenced by X-ray structures and initial in vivo efficacy.

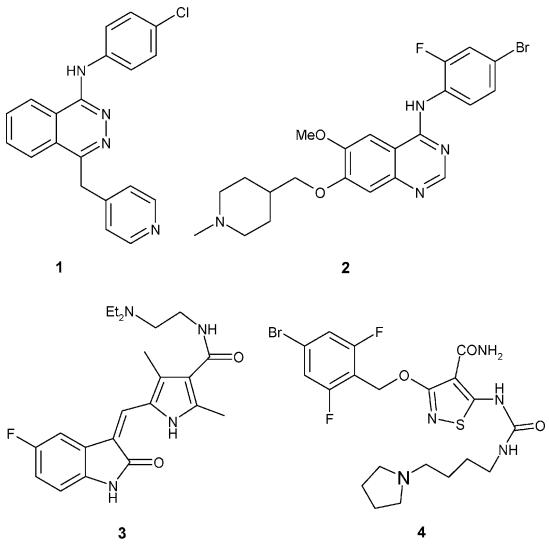

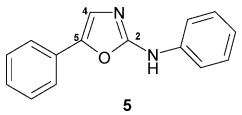

Results and Discussion

Initially we focused our investigation on the 2-anilino portion of the template, since such substitutions were easily accessible from known 2-chloro-5-phenyloxazole (**7**) via condensation with commercial anilines. As shown in Scheme 1, 2-aminoacetophenone was initially converted to 2-mercapto-5-phenyloxazole (**6**) by reaction

* Corresponding author. Phone: 919-483-6239. Fax: 919-483-6053. E-mail: Philip.A.Harris@gsk.com.

† Current addresses. M.L.B.: Eli Lilly and Co., Lilly Corporate Center, Indianapolis, IN, 46285. J.M.V.: Serenex, Inc., 323 Foster St., Durham, NC 27701. W.L.: Medtronic Vascular, 3576 Unocal Place, Santa Rosa, CA 95403. D.K.L.: MUSC, 171 Ashley Av., Charleston, SC 29425. J.A.S.: Syrrx, Inc., 10410 Science Center Drive, San Diego, CA 92121.

10.1021/jm049538w CCC: $30.25
Published on Web 02/09/2005

Scheme 1[a]

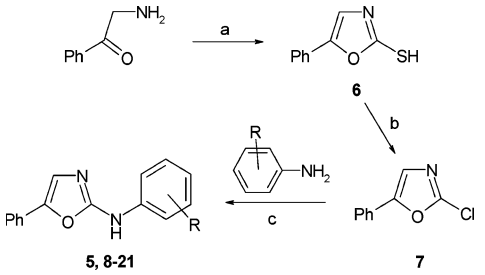

Reagents and conditions: (a) CS_2, EtOH, Na_2CO_3 (aq), 80 °C; (b) $POCl_3$, Et_3N, 100 °C; (c) ^iPrOH, 80 °C.

Table 1. Modification of the Aniline Ring

compd	R	IC_{50}, μM VEGFR2[a]	IC_{50}, μM HUVEC[b]
5	H	1.2	3.0
8	2-CN	0.87	14.4
9	2-OMe	0.38	3.26
10	3-CN	0.93	7.6
11	3-OPh	1.41	nd[c]
12	3-CH_2OH	0.50	1.65
13	3-SO_2Et	0.72	10.2
14	3-Me	0.87	1.7
15	4-SO_2NH_2	0.50	4.66
16	4-OPh	>10	nd[c]
17	3,4-di-OMe	0.14	1.13
18	3,5-di-OMe	0.17	1.69
19	3,4,5-tri-OMe	0.10	0.42
20	2-OMe, 5-SO_2NEt2	0.023	1.31
21	2-OMe, 5-SO_2Et	0.050	0.29

[a] Values are means of two or more experiments. [b] Inhibition of VEGF-induced proliferation of HUVEC cells. [c] No data.

with carbon disulfide under basic conditions,[12] and subsequent treatment with phosphorus oxychloride led to 2-chloro-5-phenyloxazole (**7**).[13]

The SAR at both enzyme and cellular levels substituting off the aniline ring is exemplified in Table 1. Monosubstitutions led only to marginal changes in enzyme and cell potencies (oxazoles **8**−**16**). Enhancements in enzymatic activity were observed by addition of methoxy groups, most prominently 3,4,5-trimethoxyanilino-5-phenyloxazole (**19**). However, significant improvements in enzyme potency were only observed from anilines combining a 2-methoxy group with either a 5-diethylsulfonamide (oxazole **20**) or 5-ethyl sulfone (oxazole **21**). Compared with the parent oxazole **5**, 2-(5-ethylsulfonyl-2-methoxyanilino)-5-phenyloxazole (**21**) yielded 25- and 10-fold enhancements in enzyme and cell potencies, respectively, and 5-ethylsulfonyl-2-methoxyaniline became the preferred aniline for SAR exploration of the 5-phenyl position. Oxazoles **9** and **13**, derived from *o*-methoxy and *m*-ethyl sulfone aniline, respectively, were only slight improvements over the parent and do not predict the efficacy of oxazole **21**. Our homology model, later supported by crystallographic data, proposed that the methoxy group sits in a lipophilic pocket and acts to orientate the sulfone group to bind to Asn 923.

To examine the SAR around the 5-phenyl ring, we employed a synthetic route previously described by Froeyen[14] whereby a variety of 2-azido-acetophenones **22** (readily available from the corresponding bromide) were converted in situ to their iminophosphoranes and condensed with 2-methoxy-5-ethyl sulfone phenylisothiocyanate (**23**) to the corresponding β-keto carbodiimides,

Scheme 2[a]

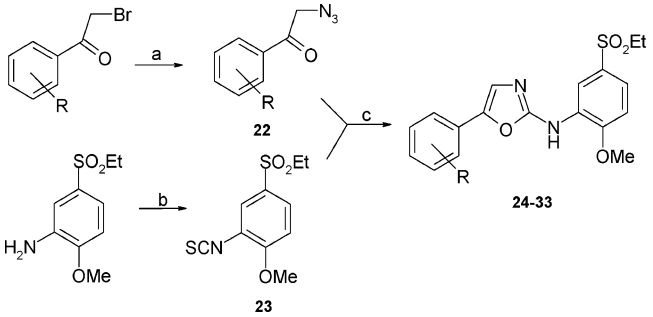

[a] Reagents and conditions: (a) NaN_3, MeOH; (b) bis(2-pyridyl)thiocarbonate, DCM or thiophosgene, $NaHCO_3$, DCM/acetone; (c) PPh_3, DCM.

Table 2. Modification of the Phenyl Ring

compd	R	IC_{50}, μM VEGFR2[a]	IC_{50}, μM HUVEC[b]
21	H	0.050	0.29
24	2-Cl	0.360	7.6
25	3-Cl	0.022	0.65
26	3-CN	0.141	1.62
27	3-MeO	0.036	1.65
28	3-F	0.093	0.35
29	4-MeO	0.087	3.20
30	4-Cl	0.081	0.93
31	4-F	0.079	0.30
32	4-CN	0.051	0.49
33	4-$CONH_2$	0.018	0.21

[a] Values are means of two or more experiments. [b] Inhibition of VEGF-induced proliferation of HUVEC cells.

which readily cyclize to the oxazoles **24**−**33** (Scheme 2). In general, ortho-substitution of the 5-phenyl ring was not favorable, whereas meta- and para-substitutions of the phenyl ring did not improve the inhibition profile compared to unsubstituted oxazole **21**, as shown in Table 2.

A homology model of the VEGFR2 enzyme, based on FGFR crystal structures, was used to predict the binding mode of the oxazole at the ATP binding site.[15,16] The Cys919 of the peptide backbone was thought to bind to the inhibitor via hydrogen donor and acceptor bonds with the anilino and oxazole nitrogens, respectively (Figure 1). As predicted from the binding mode, introduction of a methyl group at either the aniline nitrogen or the 4 position on the oxazole ring removed all VEGFR2 inhibition. The 2-methoxy-5-ethyl sulfone aniline, as mentioned earlier, was thought to impart increased potency by virtue of the methoxy substituent sitting in a small hydrophobic pocket, coupled with a sulfone oxygen accepting a hydrogen bond from the backbone nitrogen of Asn 923.

In the model, the 5-phenyl group orientates toward the back of the pocket. A vacant lipophilic pocket exists at the rear of the binding site and it was predicted that aromatic meta-substitution at the 5-phenyl ring would access this site. This region has been previously observed to be occupied by small molecule tyrosine kinase inhibitors, and interactions in this region are capable of affording distinct selectivity profiles to a given inhibitor.[15,18−20] A similar region is occupied by Gleevec in its binding to the Abl kinase, as shown in Figure 1.[17] The region to the center-right of the binding site, in the vicinity of Val 848 and Lys 868 and typically occupied by the ribose moiety of ATP, was also sterically acces-

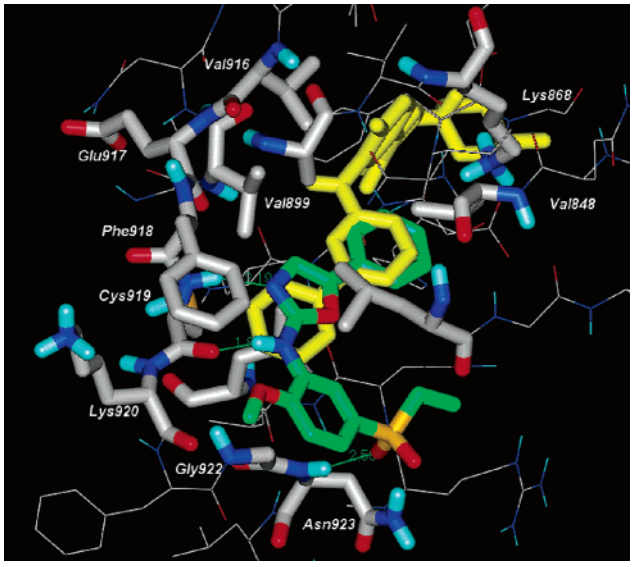

Figure 1. Predicted binding mode of oxazole **21** at the ATP binding site of the VEGFR2 kinase. The binding mode of Gleevec in Abl kinase is overlaid in yellow.[17]

Scheme 3[a]

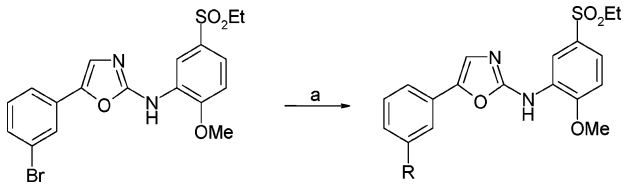

[a] Reagents and conditions: (a) $RSnBu_3$, $Pd(PPh_3)_4$, Bu_4NCl, CH_3CN, 100 °C, sealed tube.

sible. This was potentially a favorable binding site for smaller aliphatic or carbonyl groups, again via meta substitition but in the alternative orientation. To explore this a series consisting of aliphatic, carbonyl, and aromatic substituents was prepared via Stille or Suzuki palladium couplings of 5-(3-bromophenyl)oxazole **34** (Scheme 3).

Small substitutions, as exemplified by ethyl and keto derivatives **35** and **36**, did not yield inhibitors with favorable cellular activities (see Table 3). However, aromatic substitution, particularly the *o*-fluoro- or *o*-chloro-substituted phenyl groups (oxazoles **44** and **45**), resulted in inhibitors with a 7-fold increase in cellular inhibition compared with compound **21**. These oxazoles, **44** and **45**, possess the best cellular potency in this series, and evidence that their efficacy is driven by VEGFR2 inhibition is shown by a >20-fold selectivity for inhibiting VEGF- versus b-FGF-driven HUVEC proliferation.

In general, there was a moderate correlation between VEGFR2 enzyme inhibition and inhibition of HUVEC cellular proliferation, as evidenced in Figure 2, with a correlation coefficient of 0.63. A couple of outliers had good enzyme potencies but were inactive in cells (oxazoles **36** and **41**), while a couple more were somewhat more active in cells than would have been predicted from their enzyme inhibitions (oxazoles **44** and **45**). There does not appear to an easily identifiable reason for this, as the outliers have lipophilicities similar to those of others in this series and showed reasonable in vitro cell permeabilites (Papp values >50 nm/s in

Table 3. Substitution at the Meta Position of the Phenyl Ring

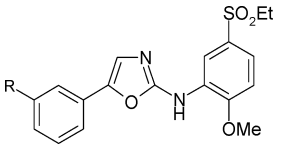

compd	R	IC_{50}, μM VEGFR2[a]	IC_{50}, μM HUVEC[b]
21	H	0.050	0.29
35	Et	0.029	1.94
36	COMe	0.091	13.90
37	2-thiophene	0.016	0.26
38	3-thiophene	0.015	0.14
39	2-pyridyl	0.022	0.37
40	3-pyridyl	0.076	0.96
41	4-pyridyl	0.078	15
42	5-(1-methylimidazole)	0.025	0.17
43	phenyl	0.079	0.11
44	2-F-phenyl	0.089	0.04
45	2-Cl-phenyl	0.039	0.05

[a] Values are means of two or more experiments. [b] Inhibition of VEGF induced proliferation of HUVEC cells.

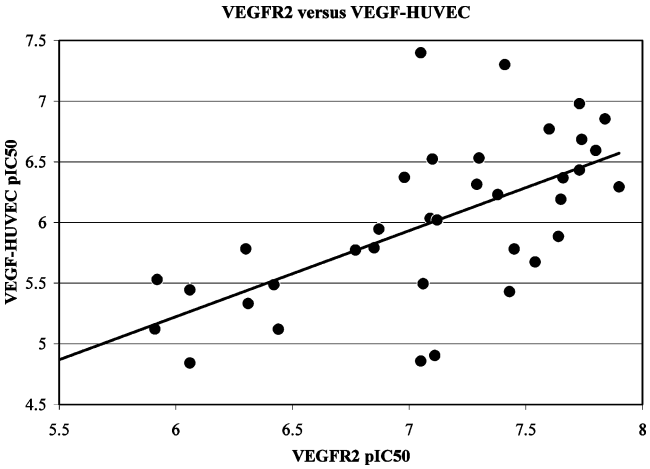

Figure 2. Correlation between pIC_{50}'s for the inhibition of VEGFR2 enzyme and VEGF-induced HUVEC cellular proliferation, $r = 0.63$.

MDCK cells with good mass balance). The average selectivity observed for VEGF- versus b-FGF-induced proliferation of HUVEC cells for compounds in this series was greater than 10-fold (see Figure 3).

Pharmacokinetics and in Vivo Efficacy. The 2-pyridyl-substituted oxazole **39** was selected on the basis of its solubility and mouse pharmacokinetic profile for in vivo evaluation in mouse xenografts. To obtain optimal exposure via oral dosing, a salt screen was conducted on oxazole **39**. In 40% SBE-β-cyclodextrin in 0.05 M methanesulfonic acid at pH 2.3, the free base had poor solubility (<1 mg/mL), which could be improved by conversion to the citrate, hydrochloride, sulfate, and tosylate salts (1−2 mg/mL). However, conversion to the mono- and bis-mesylate salts gave the best solubilities at >10 mg/mL. Oral administration to mice of an aqueous solution of the bis-mesylate salt of oxazole **39** at 100 mg/kg resulted in an AUC (0−8 h) of 102 μg h/mL with a C_{max} at 4 h of 35 μM (average of two mice). This represented an 8-fold increase in AUC compared to the free base of oxazole **39** dosed as a suspension in 0.5% HPMC with 0.1% Tween 80. The pharmacokinetics of the bis-mesylate salt of oxazole **39**

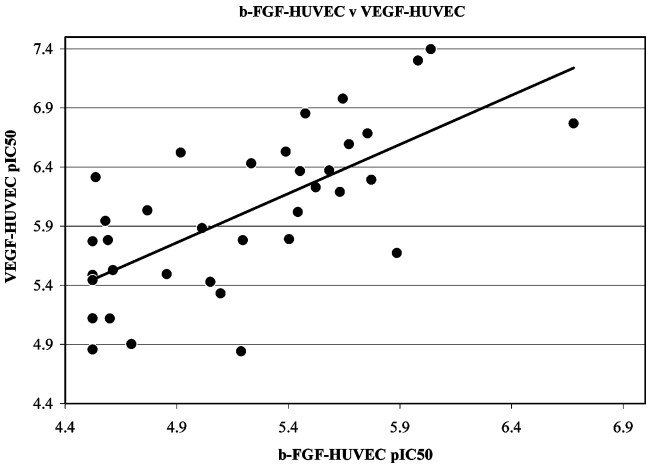

Figure 3. Correlation between pIC_{50}'s for b-FGF- and VEGF-induced HUVEC cellular proliferation, $r = 0.69$.

Table 4. Pharmacokinetic Data for Bis-mesylate Salt of Oxazole 39

PK parameter	rat[a]	dog[b]
$T_{1/2}$ (h)	1.6	3.5
Cl (mL/min/kg)	9	18
Vd_{ss} (mL/kg)	1032	3743
F (%)	11	7

[a] Average of three rats dosed at 3.5 mg/kg iv in 10% HP-β-cyclodextrin in 0.05 M acetic acid and 10 mg/kg po in 0.5% HPMC w/0.1% Tween 80. [b] Average of two dogs dosed at 1 mg/kg iv in 40% SBE-β-cyclodextrin and 1 mg/kg po in 0.5% HPMC w/0.1% Tween 80.

was further characterized in the rat and dog. The PK parameters are summarized in Table 4. Oxazole **39** showed reasonable in vitro metabolic stability data (turnover in mouse and rat S9 liver fractions after 30 min at 1 μM was 2 and 29%, respectively); thus, the low oral bioavailability is likely due to poor permeability and/or solubility, although metabolism could be a contributing factor.

In vivo efficacy was measured by the ability to inhibit the growth of established HT29 human colon tumor xenografts in nude mice. The bis-mesylate salt of oxazole **39** dosed orally once per day at either 30 or 100 mg/kg (free base equivalent) in water resulted in 43 and 55% smaller tumor, respectively, compared to vehicle control following 26 days of dosing. There was no body weight loss or other obvious signs of toxicity. By comparison, in our hands anilinoquinazoline **2** resulted in 61 and 81% inhibition of tumor growth at 30 and 100 mg/kg in the same model dosing orally once per day. As support that the observed inhibition of xenograft growth is working through an antiangiogenic rather than an antitumor mechanism, oxazole **39** has low inhibitory activity against the proliferation of HT29 cells in vitro with an IC_{50} of 4.5 μM. Inhibition of additional targets to VEGFR2 that might be contributing to the observed antiangiogenic effects such as src cannot be ruled out, although oxazole **39** is not potent against the angiogenesis-related kinases Tie-2, PDGFR, and EphB4 (see Table 6).

X-ray Crystal Structures. To confirm the binding mode of the 2-anilino-5-phenyloxazoles, the crystal structures of oxazoles **39** and **46** complexed with VEGFR2 were obtained (Table 5). The oxazole core and the 2-methoxy-5-ethyl sulfone aniline bind as predicted from the homology model, with clear density visible for the core and aniline portions in both structures. The crystal structure of oxazole **46**, possessing a *m*-3-pyridine group, showed the pyridyl group residing in the back lipophilic pocket (Figure 4). The 3-pyridyl nitrogen is proximal to the carboxylic acid of Glu885 at the rear of this pocket. No water-mediated interactions were observed; thus, the close distance implies a direct hydrogen bond via protonation of either the glutamic acid side chain or the pyridine nitrogen.

Interestingly, the crystal structure of oxazole **39** with VEGFR2 (Figure 5) shows the same core interactions, but the *m*-2-pyridine group, however, was found to be orientated in multiple conformations, with no clear density visible for this portion of the ligand. The *m*-2-pyridine appears to exist in at least two conformations, one toward the center-right position and a second conformation that projects the group into the back lipophilic pocket in a manner similar to that of oxazole **46** (Figure 4).

Given that the two X-ray structures also differ in the sulfonamide side chain (ethyl versus cyclopropyl methyl), the possibility that the *m*-3-pyridine group is driven into the back of the binding site due to steric interfer-

Table 5. Crystallographic Data

compound	39	46
space group	*P*212121	*P*212121
a (Å)	37.7	37.5
b (Å)	94.6	94.3
c (Å)	96.5	96.8
resolution range (Å)	19.8−2.1	16.6−2.1
R_{merge} (outer shell)	4.7% (37.5)	4.5% (35.5)
completeness	99.78	99.67
$I/\sigma(I)$ (outer shell)	36.6 (3.99)	42.9 (5.46)
average redundancy	6.63	6.79
no. unique reflections	20720	20768
R-factor	19.8%	19.4%
free *R* (%)	21.8%	23.8%
no. protein atoms	2098	2135
no. solvent atoms	150	151
ligand atoms	62	57
Wilson *B*-factor	36.2	36.0
average *B*-factor	38.27	39.88
rms bonded *B*-factor	1.423	1.606
rms bond lengths (Å)	0.014	0.016
rms bond angles (deg)	1.612	1.570
rms torsion angles (deg)	6.24	6.61

Table 6. Kinase Selectivity Data for Oxazoles **39**, **44** and **45**

	selectivity (μM)[a]				selectivity (μM)[a]		
kinase	**39**	**44**	**45**	kinase	39	44	45
VEGFR2	0.022	0.089	0.039	CDK2	1.7	nd	nd
VEGFR3	0.010	0.055	nd	CDK4	4.2	>10	>10
VEGFR1	0.073	0.40	0.11	GSK3	>10	>10	>10
Src	0.017	0.26	0.29	P38	>10	>10	>10
ITK	0.020	0.043	0.12	Tie-2	>10	1.4	1.8
c-FMS	0.14	0.38	1.9	EGFR	>10	>10	nd
EphB4	0.66	nd	nd	ErbB2	>10	>10	nd
PDGFR1β	1.6	0.42	0.93	PLK1	>10	nd	nd

[a] The concentration of ATP and kinase-specific biotinylated peptide in each assay was below the apparent K_m of the respective substrate. Inhibitions of VEGFR1, -2, and -3, Src, PDGFR1β, and Tie2 were evaluated by the homologous time-resolved fluorescence (HTRF) format; inhibitions of CDK2, GSK3, PLK1, EphB4, EGFR, and ErbB2 were evaluated by the scintillation proximity assay format (SPA). Inhibitions of p38 and ITK were evaluated by the fluorescence polarization (FP) binding assay. CDK4 and c-FMS inhibitions were measured by plate capture and filtration binding, respectively.

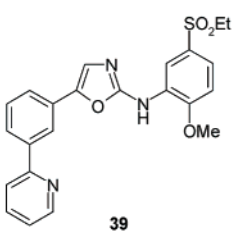

39

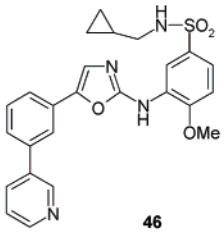

46

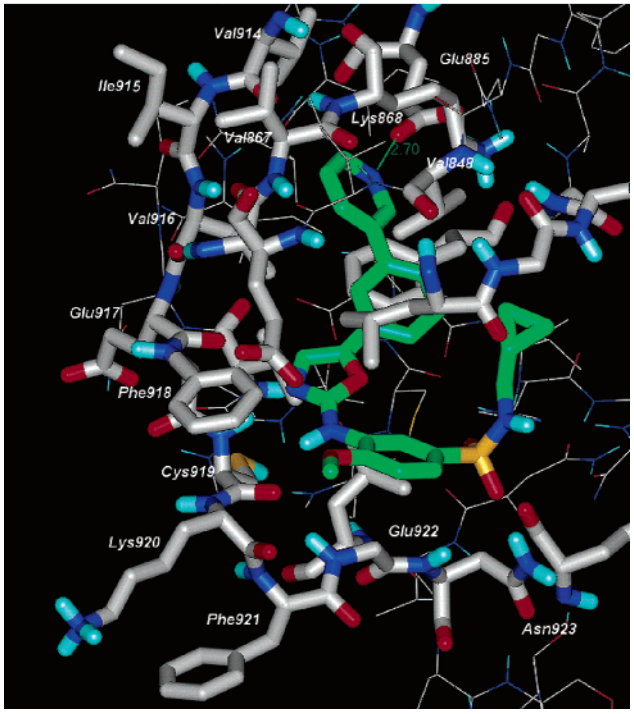

Figure 4. Crystal structure of oxazole **46** with VEGFR2.

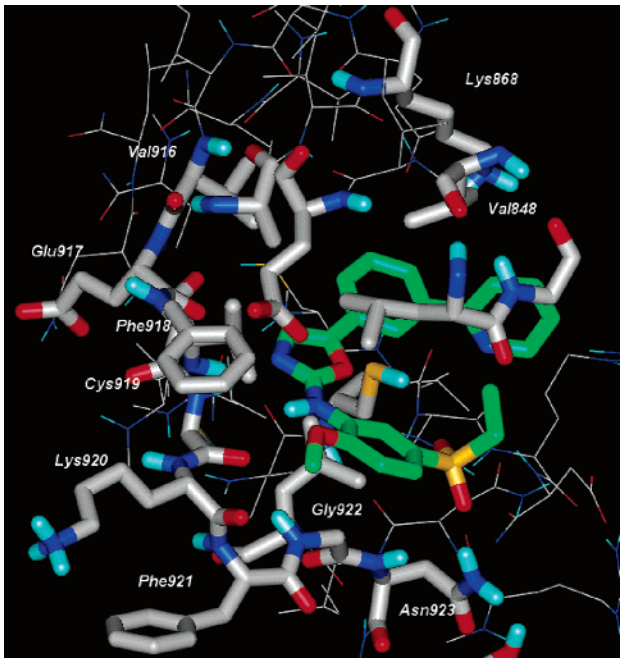

Figure 5. Crystal structure of oxazole **39** with VEGFR2. Only the conformation with the *m*-2-pyridine oriented to the center right conformation is shown.

ence with the larger cyclopropyl methyl group cannot be ruled out. However, inspection of the structures indicated that a forward conformation would be sterically allowed. Both oxazoles **39** and **46** possess similar

Table 7. Comparison of Oxazoles with VEGFR2 Clinical Candidates

	IC_{50}, μM		
compd	VEGFR2[a]	v-HUVEC[b]	b-HUVEC[c]
1	0.16	0.10	25
2	0.009	0.40	1.2
5	1.2	3.0	24
39	0.022	0.37	5.8
45	0.039	0.05	1.1

[a] Values are means of two or more experiments. [b] Inhibition of VEGF-induced proliferation of HUVEC cells. [c] Inhibition of basic FGF-induced proliferation of HUVEC cells.

IC_{50}'s for VEGFR2 inhibition of 22 and 38 nM, respectively, indicating that the energy for both binding modes is comparable. The activation loop is disordered between residues 1046 and 1065 in both crystal structures, indicating that residues beyond this region are not contributing directly to the binding affinity of these ligands. Asp1044 and Phe1045 are similarly positioned in both structures with the phenylanine side chain packing beneath the meta-substituted phenyl ring, while the aspartate side chain is facing away from the ligand, making no direct interactions.

Kinase and Cellular Selectivities. Oxazoles **39**, **44**, and **45** serve as representative examples for this series regarding selectivity against other kinases, with similar potencies against both VEGFR2 and VEGFR3 and a modest drop in potency for VEGFR1 (Table 6). Weak activities were observed for EphB4 and PDGFR1β and Tie-2, the other angiogenesis kinases assayed. Of the other kinases examined, comparable activity was seen for Src and ITK.

Evidence that cellular activity resulted from activity at the desired target was showed by comparison of the inhibition of VEGF- versus bFGF-induced proliferation of HUVEC cells. A 10-fold or better window was typically observed for this oxazole class. For example, oxazole **39** had IC_{50}'s of 0.37 and 5.8 μM for VEGF- and bFGF-induced HUVEC proliferation, respectively.

Conclusions

We have identified 2-anilino-5-aryloxazole derivatives as a novel class of potent VEGFR2 kinase inhibitors with good enzymatic and cellular activities. Optimization of both aryl rings yielded oxazole **45** with improved enzymatic and cellular inhibitions compared with unsubstituted oxazole **5** of 30- and 60-fold, respectively, and with an in vitro profile comparable to those of lead VEGFR2 inhibitors **1** and **2** now in clinical trials (see Table 7). Oxazole **39**, as the bis-mesylate salt, possessed good solubility and pharmokinetic profiles and showed moderate efficacy in preliminary in vivo xenograft studies. X-ray crystallography studies confirmed the proposed binding mode at the ATP binding site. Comparison of oxazoles **39** and **46**, differing only by a shift in position of the nitrogen on a pyridine ring from ortho to meta, revealed conformational differences in binding of the pyridine rings.

Experimental Section

All purchased starting materials were used without further purification. ^{1}H NMR spectra were recorded on a Varian VXR-300, a Varian Unity-300, or a Varian Unity-400 instrument as solutions in DMSO-d_6. Chemical shifts are expressed in parts per million (ppm, δ units). Coupling constants are in

units of hertz (Hz). Splitting patterns describe apparent multiplicities and are designated as s (singlet), d (doublet), t (triplet), q (quartet), m (multiplet), bs (broad singlet). Elemental analyses were carried out by Atlantic Microlabs Inc., Norcross, GA. **Analytical HPLC**. Method A was performed with a Beckman 166 UV detector on a Rainin Dynamex-60A column equipped with a Waters Lamda-Max 481 UV detector monitoring at 254 nm. Elution was with H_2O:MeCN:0.1% trifluoroacetic acid, with a gradient of 5−100% MeCN over 40 min. Method B was performed on a Waters analytical HPLC consisting of a 626 LC pump, 996 diode array, and a Gilson 233XL autosampler, eluting with H_2O:MeCN:0.1% formic acid with a gradient of 10−90% MeCN over 13 min, a 2 min column wash, and reequilibration period for a total of a 15 min run time (flow rate = 1.5 mL/min). LCMS using electrospray ionization were run on a Micromass ZMD mass spectrometer equipped with a Waters 2790 LC system, Phenomenex Max-RP column (4 μm, 150 × 4.60 mm), and a 996 DAD. Initial conditions, 15% MeOH (0.075% formic acid), 85% H_2O (0.1% formic acid); flow rate = 2.00 mL/min; gradient to 100% MeOH (0.075% formic acid) over 12 min, hold for 3 min, 15 min total run time.

5-Phenyl-1,3-oxazole-2-thiol (6). A solution of sodium carbonate (11.3 g, 91 mmol) in water (30 mL) was added slowly to a mixture of phenacylamine hydrochloride (15 g, 87 mmol) and carbon disulfide (13.3 g, 174 mmol) in ethanol (100 mL). After heating to 80 °C with stirring for 18 h, the reaction was cooled, filtered and treated with glacial acetic acid (25 mL), and stirred for an additional 15 min. The resulting deposited copper colored solid was collected by vacuum filtration, rinsed with ethanol, and air-dried to afford the title compound (10.84 g, 70%). ^{1}H NMR δ 13.3 (bs, 1H), 7.84 (s, 1H), 7.57 (d, J = 7.4, 2H), 7.42 (t, J = 7.5, 2H), 7.33 (t, J = 7.5, 1H); MS (ES-, m/z) = 176 (M − H)$^-$. HPLC (method A): 95% (t_R 18.4 min).

2-Chloro-5-phenyl-1,3-oxazole (7). To a suspension of 5-phenyl-1,3-oxazole-2-thiol (**6**) (11.0 g, 62 mmol) in phosphorus oxychloride (35 mL, 37.0 g, 372 mmol) cooled in an ice−water bath and under nitrogen was slowly added dry triethylamine (9.5 mL, 6.9 g, 682 mmol). The mixture was then heated to 100 °C overnight. The reaction mixture was cooled to room temperature and poured onto crushed ice. The residue was extracted with ethyl acetate (3 × 200 mL). The combined organic layers were back-washed with water, saturated sodium bicarbonate solution, and brine. The organic layer was dried over anhydrous magnesium sulfate and evaporated to leave a dark oil. The oil was purified by silica gel column chromatography using 20% ethyl acetate in hexanes as an eluant to afford the title compound (4.37 g, 39%) as an amber oil, which solidified on standing. ^{1}H NMR: δ 7.76 (s, 1H), 7.66 (d, J = 7.5, 2H), 7.46 (t, J = 7.4, 2H), 7.38 (d, J = 7.4, 1H). LCMS (ES+, m/z) = 180, 182 (MH)$^+$ (t_R 10.4 min). HPLC (method B): >99% (t_R 10.5 min).

***N*,5-Diphenyl-1,3-oxazol-2-amine (5).** A mixture of 2-chloro-5-phenyl-1,3-oxazole (**7**) (0.5 g, 2.78 mmol) and aniline (1.0 g, 10.7 mmol) was heated to 100 °C for 5 min. Upon cooling, the mixture was partitioned between ether (200 mL) and water (100 mL). The organic phase was washed with 1 N hydrochloric acid (3 × 50 mL) and then dried over anhydrous magnesium sulfate and evaporated to afford a white solid. This was then triturated with ether and filtered to yield the product as a white solid (0.18 g, 27%). ^{1}H NMR: δ 7.61 (d, J = 7.9, 2H), 7.55 (d, J = 7.5, 2H), 7.45−7.37 (m, 3H), 7.31−7.21 (m, 3H), 6.92 (t, J = 7.3, 1H). LCMS (ES+, m/z) = 237 (MH)$^+$ (t_R 10.4 min). Anal. ($C_{15}H_{12}N_2O$) C, H, N.

***N*-(2-Cyanophenyl)-5-phenyl-1,3-oxazol-2-amine Hydrochloride (8).** A mixture of 2-chloro-5-phenyl-1,3-oxazole (0.05 g, 0.28 mmol) and anthranilonitrile (0.033 g, 0.28 mmol) in 2-propanol (1.5 mL) was heated to 80 °C for 18 h with stirring. Upon cooling, a white solid precipitated out which was filtered off, washed with 2-propanol, and dried. This was then triturated with ether and filtered to yield the title product, a white solid, as the hydrochloride salt (0.045 g, 62%). Analytical purity was obtained by HPLC purification (method B) eluting with H_2O:MeCN: 0.1% formic acid; gradient 10−90% MeCN over 15 min. ^{1}H NMR: δ 11.0 (bs, 2H), 9.50 (s, 1H), 8.61 (d, J = 8.3, 1H), 8.03 (t, J = 7.4, 1H), 7.83 (d, J = 8.3, 1H), 7.77 (d, J = 7.1, 2H), 7.69 (t, J = 7.1, 1H), 7.63−7.55 (m, 4H). LCMS (ES+, m/z) = 262 (MH)$^+$ (t_R 5.2 min). Anal. ($C_{16}H_{11}N_3O$·0.2HCO_2H) C, H, N.

The following compounds **9**−**21** were similarly prepared using the appropriate aniline. In most cases, the product deposits as the hydrochloride salt; however, when the aniline has phenoxy or sulfonamide substitution, the free base is recovered.

***N*-(2-Methoxyphenyl)-5-phenyl-1,3-oxazol-2-amine Hydrochloride (9).** Tan solid; yield 87%. ^{1}H NMR: δ 9.94 (bs, 2H), 7.92 (bs, 1H), 7.60−7.55 (m, 3H), 7.42 (t, J = 7.7, 2H), 7.27 (t, J = 7.4, 1H), 7.06 (s, 2H), 6.99−6.92 (m, 1H), 3.82 (s, 3H). LCMS (ES+, m/z) = 267 (MH)$^+$ (t_R 10.8 min). HPLC (method A): 99.4% (t_R 25.2 min).

***N*-(3-Cyanophenyl)-5-phenyl-1,3-oxazol-2-amine Hydrochloride (10).** White solid; yield 50%. ^{1}H NMR: δ 10.8 (bs, 1H), 8.08 (s, 1H), 7.9 (bs, 1H), 7.82 (dd, J = 1.9, 8.3, 2H), 7.55 (d, J = 7.5, 2H), 7.48 (t, J = 8.1, 2H), 7.26−7.41 (m, 4H), 7.24 (t, J = 7.4, 1H). LCMS (ES+, m/z) = 262 (MH)$^+$ (t_R 10.2 min). Anal. ($C_{16}H_{11}N_3O$·0.1H_2O) C, H, N.

***N*-(3-Phenoxyphenyl)-5-phenyl-1,3-oxazol-2-amine (11).** White solid; yield 8%. ^{1}H NMR: δ 10.4 (s, 1H), 7.50 (d, J = 7.5, 2H), 7.36−7.41 (m, 6H), 7.28 (d, J = 7.9, 2H), 7.23 (t, J = 7.4, 1H), 7.12 (t, J = 7.4, 1H), 7.01 (d, J = 7.9, 2H), 6.55 (dd, J = 2.2, 7.2, 1H). LCMS (ES+, m/z) = 329 (MH)$^+$ (t_R 11.6 min). HPLC (method A): 99.6% (t_R 30.4 min).

***N*-(3-Hydroxymethylphenyl)-5-phenyl-1,3-oxazol-2-amine Hydrochloride (12).** White solid; yield 74%. ^{1}H NMR δ 10.44 (s, 1H), 7.58 (d, J = 6.8, 2H), 7.55 (s, 1H), 7.38−7.48 (m, 4H), 7.3 (bs, 2H), 7.21−7.27 (m, 2H), 6.89 (d, J = 7.5, 1H), 4.45 (s, 2H). LCMS (ES+, m/z) = 267 (MH)$^+$ (t_R 9.0 min). HPLC (method A): >99% (t_R 17.6 min).

***N*-(3-(Ethylsulfonyl)phenyl)-5-phenyl-1,3-oxazol-2-amine (13).** White solid; yield 37%. ^{1}H NMR: δ 10.86 (s, 1H), 8.34 (s, 1H), 7.92 (dd, J = 1.6, 8.0, 1H), 7.61−7.67 (m, 3H), 7.57 (s, 1H), 7.46−7.51 (m, 3H), 7.33 (t, J = 7.3, 1H), 3.30 (q, J = 7.3, 2H), 1.16 (t, J = 7.3, 3H). LCMS (ES+, m/z) = 329 (MH)$^+$ (t_R 9.3 min). HPLC (method B): >99% (t_R 10.5 min).

***N*-(3-Methylphenyl)-5-phenyl-1,3-oxazol-2-amine (14).** White solid; yield 14%; initially deposited as the hydrochloride salt and converted to the free base by partitioning between ethyl acetate and aqueous sodium bicarbonate. ^{1}H NMR: δ 10.18 (s, 1H), 7.53 (d, J = 7.5, 2H), 7.43−7.34 (m, 4H), 7.21 (t, J = 7.4, 1H), 7.13 (t, J = 7.8, 1H), 6.92 (d, J = 7.5, 1H), 2.24 (s, 3H). LCMS (ES+, m/z) = 251 (MH)$^+$ (t_R 11.3 min). Anal. ($C_{16}H_{14}N_2O$) C, H, N.

4-[(5-Phenyl-1,3-oxazol-2-yl)amino]benzenesulfonamide (15). White solid; yield 64%. ^{1}H NMR: δ 10.77 (s, 1H), 7.74 (s, 4H), 7.58 (d, J = 7.5, 2H), 7.50 (s, 1H), 7.42 (t, J = 7.7, 2H), 7.26 (t, J = 7.4, 1H), 7.17 (s, 2H). LCMS (ES+, m/z) = 316 (MH)$^+$ (t_R 8.3 min). HPLC (method A): 99.0% (t_R 21.1 min).

***N*-(4-Phenoxyphenyl)-5-phenyl-1,3-oxazol-2-amine (16).** White solid; yield 50%. ^{1}H NMR: δ 10.38 (s, 1H), 7.64 (d, J = 9.1, 2H), 7.57 (d, J = 7.4, 2H), 7.23−7.46 (m, 6H), 7.01−7.09 (m, 3H), 6.93 (d, J = 7.9, 2H). LCMS (ES+, m/z) = 329 (MH)$^+$ (t_R 11.6 min). Anal. ($C_{21}H_{16}N_2O_2$·0.5H_2O) C, H, N.

***N*-(3,4-Dimethoxyphenyl)-5-phenyl-1,3-oxazol-2-amine Hydrochloride (17).** White solid; yield 53%. ^{1}H NMR: δ 10.55 (s, 1H), 7.57−7.53 (m, 3H), 7.41 (t, J = 7.8, 2H), 7.31−7.23 (m, 2H), 7.07 (dd, J = 2.4, 8.6, 1H), 6.91 (d, J = 8.8, 1H), 3.73 (s, 3H), 3.69 (s, 3H). LCMS (ES+, m/z) = 297 (MH)$^+$ (t_R 9.6 min). HPLC (method A): >99% (t_R 21.8 min).

***N*-(3,5-Dimethoxyphenyl)-5-phenyl-1,3-oxazol-2-amine Hydrochloride (18).** White solid; yield 43%. ^{1}H NMR: δ 10.27 (s, 1H), 7.52 (d, J = 7.5, 2H), 7.42 (s, 1H), 7.38 (t, J = 7.7, 2H), 7.22 (t, J = 7.4, 1H), 6.83 (d, J = 2.0, 2H), 6.08 (t, J = 2.0, 1H), 3.68 (s, 6H). LCMS (ES+, m/z) = 297 (MH)$^+$ (t_R 10.4 min). Anal. ($C_{17}H_{16}N_2O_3$·0.35H_2O) C, H, N.

***N*-(3,4,5-Trimethoxyphenyl)-5-phenyl-1,3-oxazol-2-amine hydrochloride (19).** White solid; yield 17%. ^{1}H NMR: δ 10.23 (s, 1H), 7.52 (d, J = 7.5, 2H), 7.43 (s, 1H), 7.38 (t, J = 7.8, 2H), 7.22 (t, J = 7.4, 1H), 6.96 (s, 2H), 3.71 (s, 6H),

3.56 (s, 3H). LCMS (ES+, *m/z*) = 327 $(MH)^+$ (t_R 9.9 min). Anal. ($C_{18}H_{18}N_2O_4 \cdot 0.1H_2O$) C, H, N.

***N,N*-Diethyl-4-methoxy-3-[(5-phenyl-1,3-oxazol-2-yl)-amino]benzenesulfonamide (20).** White solid; yield 40%. ^{1}H NMR: δ 9.46 (s, 1H), 8.69 (d, J = 2.2, 1H), 7.58 (d, J = 7.3, 2H), 7.50 (s, 1H), 7.44−7.35 (m, 3H), 7.25 (t, J = 7.4, 1H), 7.16 (d, J = 8.6, 1H), 3.92 (s, 3H), 3.12 (q, J = 7.1, 4H), 1.02 (t, J = 7.1, 6H). LCMS (ES+, *m/z*) = 402 $(MH)^+$ (t_R 10.5 min). HPLC (method A): 99.5% (t_R 28.6 min).

***N*-[5-(Ethylsulfonyl)-2-methoxyphenyl]-5-phenyl-1,3-oxazol-2-amine (21).** White solid; yield 26%. ^{1}H NMR: δ 9.72 (s, 1H), 8.75 (d, J = 2.2, 1H), 7.59 (d, J = 7.5, 2H), 7.51 (s, 1H), 7.46 (dd, J = 2.2, 8.4, 1H), 7.41 (t, J = 7.8, 2H), 7.29−7.22 (m, 2H), 3.94 (s, 3H), 3.17 (q, J = 7.4, 2H), 1.08 (t, J = 7.4, 3H). LCMS (ES+, *m/z*) = 359 $(MH)^+$ (t_R 9.3 min). HPLC (method A): 98.6% (t_R 25.1 min).

General Procedure for Preparation of 2-Azidoacetophenones (22). To a solution of the phenacyl bromide (73 mmol) in methanol (150 mL) was added sodium azide (5.42 g, 83 mmol) and the reaction stirred at room temperature for 90 min. The solvent was removed under reduced pressure and the crude product was partitioned between ethyl acetate (200 mL) and water (100 mL). The organic layer was separated, dried over anhydrous magnesium sulfate, and concentrated under reduced pressure to afford the 2-azidoacetophenones **22**.

4-(Ethylsulfonyl)-2-isothiocyanato-1-methoxybenzene (23). A solution of 5-(ethylsulfonyl)-2-methoxyaniline (15.6 g, 72.5 mmol) in dichloromethane (100 mL) was added dropwise over 1 h to a stirred solution of thiophosgene (9 g, 78.0 mmol) in dichloromethane (300 mL) at room temperature. After the addition was complete, the reaction was stirred for 2 h. Subsequently, saturated aqueous sodium bicarbonate (200 mL) was added, and the reaction was stirred for an additional 1 h. The organic layer was separated, and the aqueous layer was extracted with dichloromethane (2 × 100 mL). The combined organic layers were dried over anhydrous magnesium sulfate, filtered, and concentrated under reduced pressure to afford the title compound **23** (18.6 g, 72.4 mmol) as a tan solid. ^{1}H NMR: δ 7.78 (dd, J = 2.2, 8.8, 1H), 7.71 (d, J = 2.2, 1H), 7.35 (d, J = 8.8, 1H), 3.95 (s, 3H), 3.22 (q, J = 7.4, 2H), 1.02 (t, J = 7.3, 3H). Anal. ($C_{10}H_{11}NO_3S_2$) C, H, N, S.

General Procedure for the Preparation of 5-(Substituted-phenyl)-*N*-[5-(ethylsulfonyl)-2-methoxyphenyl]-1,3-oxazol-2-amines (24−33). A solution of the 2-azidoacetophenone **(22)** (72.5 mmol) in dichloromethane (50 mL) was added dropwise over 2 h to a stirred solution of the isothiocyanate **23** (18.6 g, 72.4 mmol) and triphenylphosphine (18.8 g, 73 mmol) in dichloromethane (100 mL) under nitrogen. The reaction was kept cool during the addition by periodically placing the flask in an ice water bath. After the addition was complete, the reaction was stirred at room temperature for an additional 2 h. Subsequently, oxalic acid (6.5 g, 72.0 mmol) was added, and the reaction was briefly warmed with a heat gun until the appearance of a precipitate. After cooling in ice water, the precipitate was filtered, washed with dichloromethane and diethyl ether, and partitioned between dichloromethane (200 mL) and 1 M aqueous sodium hydroxide (100 mL). The organic layer was separated, and the aqueous layer was extracted with additional dichloromethane (2 × 100 mL). The combined organic layers were dried over anhydrous magnesium sulfate, filtered, and concentrated under reduced pressure to afford the desired compound. In cases where the addition of oxalic acid did not yield a precipitate, the solution was subsequently diluted with diethyl ether (100 mL) and extracted with 6 N hydrochloric acid (100 mL). The aqueous phase was separated, basified by addition of 5 N sodium hydroxide solution, and extracted with ethyl acetate (3 × 100 mL). The combined organic layers were dried over anhydrous magnesium sulfate, filtered, and concentrated under reduced pressure to afford the crude compound. Purification was achieved either by trituration with methanol, filtering off the precipitate and washing with methanol, or by flash chromatography on silica gel with hexanes/EtOAc.

5-(2-Chlorophenyl)-N-[5-(ethylsulfonyl)-2-methoxyphenyl]-1,3-oxazol-2-amine (24). Yellow solid; yield 25%. ^{1}H NMR: δ 9.90 (s, 1H), 8.80 (s, 1H), 7.78 (d, J = 7.7, 1H), 7.73 (s, 1H), 7.47−7.61 (m, 3H), 7.30−7.38 (m, 2H), 4.01 (s, 3H), 3.23 (q, J = 7.3, 2H), 1.14 (t, J = 7.3, 3H). LCMS (ES+, *m/z*) = 393 $(MH)^+$ (t_R 10.1 min). HPLC (method B): >95% (t_R 12.7 min).

5-(3-Chlorophenyl)-*N*-[5-(ethylsulfonyl)-2-methoxyphenyl]-1,3-oxazol-2-amine (25). Off-white solid; yield 3%. ^{1}H NMR: δ 9.77 (s, 1H), 8.72 (d, J = 2.1, 1H), 7.63 (m, 2H), 7.51 (d, J = 7.9, 1H), 7.45 (dd, J = 2.2, 8.6, 1H), 7.41 (d, J = 7.9, 1H), 7.28 (d, J = 8.2, 1H), 7.22 (d, J = 8.6, 1H), 3.93 (s, 3H), 3.15 (q, J = 7.3, 2H), 1.06 (t, J = 7.3, 3H). LCMS (ES+, *m/z*) = 393 $(MH)^+$ (t_R 10.2 min). HPLC (method B): >95% (t_R 11.5 min).

5-(3-Cyanophenyl)-*N*-[5-(ethylsulfonyl)-2-methoxyphenyl]-1,3-oxazol-2-amine (26). Yellow solid; yield 1%. ^{1}H NMR: δ 9.80 (s, 1H), 8.71 (d, J = 2.2, 1H), 8.01 (s, 1H), 7.84 (d, J = 7.9, 1H), 7.69−7.63 (m, 2H), 7.61 (t, J = 7.9, 1H), 7.46 (dd, J_1=8.5, J_2=2.2, 1H), 7.23 (d, J = 8.5, 1H), 3.93 (s, 3H), 3.16 (q, J = 7.3, 2H), 1.06 (t, J = 7.3, 3H). LCMS (ES+, *m/z*) = 384 $(MH)^+$ (t_R 8.6 min). HPLC (method B): >95% (t_R 10.1 min).

5-(3-Methoxyphenyl)-*N*-[5-(ethylsulfonyl)-2-methoxyphenyl]-1,3-oxazol-2-amine (27). Off-white solid; yield 49%. ^{1}H NMR: δ 9.71 (s, 1H), 8.74 (d, J = 2.2, 1H), 7.53 (s, 1H), 7.46 (dd, J = 2.2, 8.6, 1H), 7.32 (t, J = 8.0, 1H), 7.24 (d, J = 8.6, 1H), 7.17 (d, J = 7.7, 1H), 7.13 (s, 1H), 6.83 (dd, J = 2.4, 8.2, 1H), 3.94 (s, 3H), 3.78 (s, 3H), 3.17 (q, J = 7.3, 2H), 1.08 (t, J = 7.3, 3H). LCMS (ES+, *m/z*) = 389 $(MH)^+$ (t_R 9.5 min). HPLC (method A): 95.6% (t_R 24.4 min).

5-(3-Fluorophenyl)-*N*-[5-(ethylsulfonyl)-2-methoxyphenyl]-1,3-oxazol-2-amine oxalate (28). Off-white solid; yield 27%. ^{1}H NMR: δ 9.75 (bs, 1H), 8.71 (d, J = 2.2, 1H), 7.59 (s, 1H), 7.47−7.36 (m, 4H), 7.22 (d, J = 8.6, 1H), 7.08−7.04 (m, 1H), 3.92 (s, 3H), 3.15 (q, J = 7.3, 2H), 1.06 (t, J = 7.3, 3H). LCMS (ES+, *m/z*) = 377 $(MH)^+$ (t_R 9.5 min). HPLC (method B): >95% (t_R 10.8 min).

5-(4-Methoxyphenyl)-*N*-[5-(Ethylsulfonyl)-2-methoxyphenyl]-1,3-oxazol-2-amine Hydrochloride (29). White solid; yield 58%. ^{1}H NMR: δ 9.68 (s, 1H), 8.72 (d, J = 2.2, 1H), 7.46 (dd, J = 2.2, 8.6, 1H), 7.35 (s, 1H), 7.22 (d, J = 8.4, 1H), 6.99 (d, J = 8.8, 2H), 5.0 (bs, 1H), 3.94 (s, 3H), 3.76 (s, 3H), 3.17 (q, J = 7.3, 2H), 1.08 (t, J = 7.4, 3H). LCMS (ES+, *m/z*) = 389 $(MH)^+$ (t_R 9.3 min). HPLC (method A): 92.7% (t_R 25.1 min).

5-(4-Chlorophenyl)-*N*-[5-(ethylsulfonyl)-2-methoxyphenyl]-1,3-oxazol-2-amine (30). Off-white solid; yield 10%. ^{1}H NMR: δ 9.91 (bs, 1H), 8.69 (d, J = 2.2, 1H), 7.85 (d, J = 8.3 Hz, 2H), 7.77 (s, 1H), 7.70 (d, J = 8.3, 2H), 7.47 (dd, J = 2.2, 8.7, 1H), 7.23 (d, J = 8.7, 1H), 3.92 (s, 3H), 3.16 (q, J = 7.3, 2H), 1.06 (t, J = 7.3, 3H). LCMS (ES+, *m/z*) = 393 $(MH)^+$ (t_R 10.1 min). HPLC (method B): >95% (t_R 11.5 min).

5-(4-Fluorophenyl)-*N*-[2-methoxy-5-(methylsulfonyl)-phenyl]-1,3-oxazol-2-amine Hydrochloride (31). White solid; yield 19%. ^{1}H NMR: δ 9.8 (bs, 1H), 8.70 (d, J = 2.2, 1H), 7.60−7.64 (m, 2H), 7.51 (s, 1H), 7.48 (dd, J = 2.2, 8.6, 1H), 7.23−7.30 (m, 3H), 3.94 (s, 3H), 3.17 (q, J = 7.3, 2H), 1.08 (t, J = 7.3, 3H), LCMS (ES+, *m/z*) = 377 $(MH)^+$ (t_R 9.4 min). HPLC (method A): >99% (t_R 26.2 min).

5-(4-Cyanophenyl)-*N*-[5-(ethylsulfonyl)-2-methoxyphenyl]-1,3-oxazol-2-amine (32). Off-white solid; yield 6%. ^{1}H NMR: δ 9.91 (bs, 1H), 8.69 (d, J = 2.2, 1H), 7.85 (d, J = 8.3, 2H), 7.77 (s, 1H), 7.70 (d, J = 8.3, 2H), 7.47 (dd, J = 2.2, 8.7, 1H), 7.23 (d, J = 8.7, 1H), 3.92 (s, 3H), 3.16 (q, J = 7.3, 2H), 1.06 (t, J = 7.3, 3H). LCMS (ES+, *m/z*) = 384 $(MH)^+$ (t_R 8.6 min). HPLC (method B): >95% (t_R 10.0 min).

4-(2-{[5-(Ethylsulfonyl)-2-methoxyphenyl]amino}-1,3-oxazol-5-yl)benzamide (33). 5-(4-Cyanophenyl)-*N*-[5-(ethylsulfonyl)-2-methoxyphenyl]-1,3-oxazol-2-amine (**32**) (0.084 g, 0.22 mmol) was treated with concentrated hydrochloric acid (4 mL) and stirred at room temperature overnight. The reaction mixture was diluted with ethyl acetate and made basic with 5 N sodium hydroxide solution. The aqueous layer

was extracted with ethyl acetate (3 × 10 mL). The combined organic layers were dried over anhydrous magnesium sulfate, filtered, and evaporated under reduced pressure to afford the title compound (0.085 g, 97% yield) as a yellow solid. ^{1}H NMR: δ 9.78 (bs, 1H), 8.72 (d, J = 2.1, 1H), 7.94 (s, 1H), 7.89 (d, J = 8.2, 2H), 7.63−7.61 (m, 3H), 7.46 (dd, J = 2.1, 8.6, 1H), 7.32 (s, 1H), 7.22 (d, J = 8.6, 1H), 3.93 (s, 3H), 3.15 (q, J = 7.3, 2H), 1.07 (t, J = 7.3, 3H). LCMS (ES+, m/z) = 402 (MH)$^+$ (t_R 7.1 min). HPLC (method B): >95% (t_R 7.6 min).

5-(3-Bromophenyl)-*N*-[5-(ethylsulfonyl)-2-methoxyphenyl]-1,3-oxazol-2-amine (34). The title compound was prepared as described earlier in the general procedure for the preparation of 5-(substituted-phenyl)-*N*-[5-(ethylsulfonyl)-2-methoxyphenyl]-1,3-oxazol-2-amines; yellow solid, yield 36%. ^{1}H NMR: δ 9.77 (s, 1H), 8.72 (d, J = 2.2, 1H), 7.77 (s, 1H), 7.62 (s, 1H), 7.56 (d, J = 7.9, 1H), 7.47−7.33 (m, 3H), 7.22 (d, J = 8.6, 1H), 3.93 (s, 3H), 3.17 (q, J = 7.3, 2H), 1.06 (t, J = 7.3, 3H). LCMS (ES+, m/z) = 437, 439 (MH)$^+$ (t_R 10.3 min). Anal. ($C_{18}H_{17}N_2BrO_4S$) C, H, N, Br, S.

General Procedure for the Stille Coupling of 5-(3-Bromophenyl)-*N*-[5-(ethylsulfonyl)-2-methoxyphenyl]-1,3-oxazol-2-amine. In a Pyrex sealed tube, oxazole **34** (0.123 g, 0.28 mmol), the appropriate tributylstannyl reagent (1 mmol), tetrabutylammonium chloride (0.170 g, 0.61 mmol), and tetrakistriphenylphosphine palladium(0) (0.02 g, 0.017 mmol) were suspended in dry acetonitrile (10 mL) and stirred at 100 °C. After the reaction was determine to be complete by TLC analysis, the reaction was cooled, diluted with ethyl acetate (50 mL), quenched with 1 M aqueous potassium fluoride solution (20 mL), and stirred for 3 h. The organic layer was separated, dried over anhydrous magnesium sulfate, filtered, and concentrated under reduced pressure. The crude product was purified by column chromatography on silica gel eluting with hexane:ethyl acetate to afford the desired compound.

Preparation of 5-(3-Ethylphenyl)-*N*-[5-(ethylsulfonyl)-2-methoxyphenyl]-1,3-oxazol-2-amine (35). 5-(3-Vinylphenyl)-*N*-[5-(ethylsulfonyl)-2-methoxyphenyl]-1,3-oxazol-2-amine was prepared by the Stille coupling procedure described above as a red-brown solid in 73% yield. ^{1}H NMR: δ 9.69 (s, 1H), 8.72 (d, J = 2.2, 1H), 7.66 (s, 1H), 7.36−7.55 (m, 5H), 7.22 (d, J = 8.6, 1H), 6.72 (dd, J = 11.2, 17.5, 1H), 5.86 (d, J = 17.6, 1H), 5.29 (d, J = 11.2, 1H), 3.93 (s, 3H), 3.15 (q, J = 7.3, 2H), 1.06 (t, J = 7.3, 3H). MS (ES+, m/z) = 385 (MH)$^+$ (t_R 10.7 min). The solid (0.049 g, 013 mmol) was dissolved in ethyl acetate (15 mL), and 10% palladium on carbon (0.018 g) added. The reaction mixture was placed under hydrogen at 40 psi and shaken for 3 h. The reaction mixture was filtered through Celite and purified by flash chromatography on silica gel with hexanes/EtOAc (2/1) to yield the title compound as an off-white solid (0.035 g, 70%). ^{1}H NMR: δ 9.68 (s, 1H), 8.73 (d, J = 2.0, 1H), 7.44−7.48 (m, 3H), 7.40 (d, J = 7.7, 1H), 7.32 (t, J = 7.5, 1H), 7.23 (d, J = 7.6, 1H), 7.10 (d, J = 7.5, 1H), 3.94 (s, 3H), 3.18 (q, J = 7.3, 2H), 2.60 (q, J = 7.6, 2H), 1.18 (t, J = 7.6, 3H), 1.08 (t, J = 7.3, 3H). LCMS (ES+, m/z) = 387 (MH)$^+$ (t_R 10.7 min). HPLC (method B): >99% (t_R 11.8 min).

1-[3-(2-{[5-(Ethylsulfonyl)-2-methoxyphenyl]amino}-1,3-oxazol-5-yl)phenyl]ethanone (36). 5-(3-Oxazole **34** (2 g, 4.6 mmol), 1-ethoxyvinyltribuyltin (2 g, 5.52 mmol), tetrabutylammonium chloride (2.66 g, 9.6 mmol), and tetrakistriphenylphosphine palladium(0) (0.5 g, 0.43 mmol) were suspended in DMF (50 mL) and stirred at 110 °C under nitrogen. After 1 h the reaction was cooled and evaporated under reduced pressure. The crude residue was partitioned between 3:1 diethyl ether/dichloromethane (100 mL) and 1 N hydrochloric acid (100 mL) and stirred for 1 h. The resulting precipitate was filtered off, washed with diethyl ether followed by water, and dried to yield the title compound as a tan solid (1.45 g, 79%). ^{1}H NMR: δ 9.90 (s, 1H), 8.81 (d, J = 2.3, 1H), 8.18 (s, 1H), 7.90 (d, J = 9.2, 2H), 7.72 (s, 1H), 7.63 (t, J = 8.0, 1H), 7.52 (dd, J = 2.3, 6.3, 1H), 7.31 (d, J = 8.5, 1H), 4.01 (s, 3H), 3.24 (q, J = 7.3, 2H), 2.66 (s, 3H), 1.15 (t, J = 7.3, 3H). LCMS (ES+, m/z) = 401 (MH)$^+$ (t_R 8.8 min). Anal. ($C_{20}H_{20}N_2O_5S$·0.4H_2O) C, H, N, S.

Compounds **37**−**43** were prepared following the general Stille coupling procedure described above.

***N*-[5-(Ethylsulfonyl)-2-methoxyphenyl]-5-(3-thien-2-ylphenyl)-1,3-oxazol-2-amine (37).** White solid; yield 20%. ^{1}H NMR: δ 9.76 (s, 1H), 8.74 (d, J = 2.2, 1H), 7.82 (s, 1H), 7.60 (s, 1H), 7.50−7.56 (m, 4H), 7.41−7.46 (m, 2H), 7.22 (d, J = 8.5, 1H), 7.13 (t, J = 3.8, 1H), 3.94 (s, 3H), 3.16 (q, J = 7.4, 2H), 1.07 (t, J = 7.3, 3H). LCMS (ES+, m/z) = 441 (MH)$^+$ (t_R 11.0 min). HPLC (method B): >99% (t_R 12.6 min).

***N*-[5-(Ethylsulfonyl)-2-methoxyphenyl]-5-(3-thien-3-ylphenyl)-1,3-oxazol-2-amine (38).** Off-white solid; yield 52%. ^{1}H NMR: δ 9.80 (bs, 1H), 8.81 (s, 1H), 7.98 (s, 2H), 7.60−7.75 (m, 4H), 7.46−7.60 (m, 3H), 7.31 (d, J = 8.6, 1H), 4.01 (s, 3H), 3.24 (q, J = 7.4, 2H), 1.15 (t, J = 7.3, 3H). LCMS (ES+, m/z) = 441 (MH)$^+$ (t_R 10.9 min). HPLC (method B): >99% (t_R 12.4 min).

***N*-[5-(Ethylsulfonyl)-2-methoxyphenyl]-5-(3-pyridin-2-ylphenyl)-1,3-oxazol-2-amine (39).** White solid; yield 51%. ^{1}H NMR: δ 9.79 (s, 1H), 8.76 (d, J = 2.2, 1H), 8.65 (d, J = 4.2, 1H) 8.32 (s, 1H), 7.98 (d, J = 7.9, 1H), 7.94 (d, J = 7.9, 1H), 7.88 (dt, J = 1.6, 7.5, 1H), 7.65 (d, J = 7.9, 1H), 7.60 (s, 1H), 7.51 (t, J = 7.9, 1H), 7.45 (dd, J = 2.2, 8.6, 1H), 7.36 (dd, J = 2.0, 7.1, 1H), 7.22 (d, J = 8.6, 1H), 3.94 (s, 3H), 3.16 (q, J = 7.3, 2H), 1.07 (t, J = 7.3, 3H). LCMS (ES+, m/z) = 436 (MH)$^+$ (t_R 9.1 min). Anal. ($C_{23}H_{21}N_3O_4S$·0.25H_2O) C, H, N, S.

***N*-[5-(Ethylsulfonyl)-2-methoxyphenyl]-5-(3-pyridin-3-ylphenyl)-1,3-oxazol-2-amine (40).** White solid; yield 49%. ^{1}H NMR: δ 9.74 (s, 1H), 9.08 (s, 1H), 8.72 (s, 2H), 8.44−8.52 (m, 1H), 7.98 (s, 1H), 7.70−7.84 (m, 1H), 7.64−7.68 (m, 3H), 7.58 (d, J = 7.5, 1H), 7.46 (d, J = 8.2, 1H), 7.22 (d, J = 8.6, 1H), 3.93 (s, 3H), 3.16 (q, J = 7.3, 2H), 1.06 (t, J = 7.3, 3H). LCMS (ES+, m/z) = 436 (MH)$^+$ (t_R 8.5 min). HPLC (method B): >99% (t_R 7.2 min).

***N*-[5-(Ethylsulfonyl)-2-methoxyphenyl]-5-(3-pyridin-4-ylphenyl)-1,3-oxazol-2-amine (41).** Tan solid; yield 34%. ^{1}H NMR: δ 9.73 (s, 1H), 8.74 (d, J = 2.2, 1H), 8.63 (d, J = 6.1, 2H) 7.97 (s, 1H), 7.71 (d, J = 6.1, 2H), 7.64−7.68 (m, 3H), 7.55 (t, J = 7.7, 1H), 7.44 (dd, J = 2.2, 8.5, 1H), 7.23 (d, J = 8.6, 1H), 3.93 (s, 3H), 3.17 (q, J = 7.3, 2H), 1.07 (t, J = 7.3, 3H). LCMS (ES+, m/z) = 436 (MH)$^+$ (t_R 7.9 min). HPLC (method B): >99% (t_R 6.1 min).

***N*-[5-(Ethylsulfonyl)-2-methoxyphenyl]-5-[3-(1-methyl-1*H*-imidazol-5-yl)phenyl]-1,3-oxazol-2-amine (42).** Off-white solid; yield 28%. ^{1}H NMR: δ 9.71 (s, 1H), 8.73 (d, J = 2.0, 1H), 7.68 (d, J = 9.7, 2H), 7.59 (s, 1H), 7.55 (d, J = 7.5, 1H), 7.45 (m, 2H), 7.35 (d, J = 7.7, 1H), 7.22 (d, J = 7.4, 1H), 7.07 (s, 1H), 3.93 (s, 3H), 3.67 (s, 3H), 3.15 (q, J = 7.3, 2H), 1.06 (t, J = 7.3, 3H). LCMS (ES+, m/z) = 439 (MH)$^+$ (t_R 5.2 min). HPLC (method B): >95% (t_R 5.1 min).

5-(1,1′-Biphenyl-3-yl)-*N*-[5-(ethylsulfonyl)-2-methoxyphenyl]-1,3-oxazol-2-amine (43). Off-white solid; yield 49%. ^{1}H NMR: δ 9.72 (s, 1H), 8.74 (d, J = 2.4, 1H), 7.85 (s, 1H), 7.67 (d, J = 7.3, 2H), 7.61 (s, 1H), 7.44−7.58 (m, 6H), 7.37 (t, J = 6.2, 1H), 7.22 (d, J = 8.6, 1H), 3.93 (s, 3H), 3.15 (q, J = 7.3, 2H), 1.06 (t, J = 7.3, 3H). LCMS (ES+, m/z) = 435 (MH)$^+$ (t_R 11.2 min). Anal. ($C_{24}H_{22}N_2O_4S$) C, H, N, S.

***N*-[5-(Ethylsulfonyl)-2-methoxyphenyl]-5-(2′-fluoro-1,1′-biphenyl-3-yl)-1,3-oxazol-2-amine (44).** In a Pyrex sealed tube, a mixture of oxazole **34** (0.1 g, 0.23 mmol), 2-fluorophenylboronic acid (0.048 g, 0.34 mmol), anhydrous lithium chloride (0.029 g, 0.68 mmol), (bistriphenylphosphine)palladium(II) chloride (0.016 g, 0.023 mmol), and 2 M aqueous sodium carbonate solution (0.29 mL, 0.58 mmol) was suspended in 1:1 ethanol/dichloromethane (2 mL). The reaction mixture was stirred at 100 °C for 16 h. The crude product was partitioned between ethyl acetate (50 mL) and 1 N sodium hydroxide (50 mL). The organic layer was separated, dried over anhydrous magnesium sulfate, filtered, and concentrated under reduced pressure. The product was purified by preparative plate chromatography eluting with hexane:ethyl acetate (60−80%) to afford the title compound (0.045 g, 44%) as a peach solid. An Analytical purity was obtained by HPLC purification (method B) eluting with H_2O:MeCN:0.1% formic acid, gradient 10−90% MeCN over 15 min. ^{1}H NMR: δ 9.82

(s, 1H), 8.82 (d, $J = 2.1$, 1H), 7.82 (s, 1H), 7.70−7.34 (m, 9H), 7.30 (d, $J = 8.6$, 1H), 4.00 (s, 3H), 3.23 (q, $J = 7.3$, 2H), 1.14 (t, $J = 7.3$, 3H). LCMS (ES+, m/z) = 453 $(MH)^+$ (t_R 10.7 min). Anal. ($C_{24}H_{21}FN_2O_4S \cdot 0.6HCO_2H$) C, H, N, S.

***N*-[5-(Ethylsulfonyl)-2-methoxyphenyl]-5-(2′-chloro-1,1′-biphenyl-3-yl)-1,3-oxazol-2-amine (45).** Following the same procedure described for the preparation of **44,** substituting 2-chloroboronic acid afforded the title compound (0.022 g, 21%) as an off-white solid. ^{1}H NMR: δ 9.80 (bs, 1H), 8.81 (s, 1H), 7.69−7.49 (m, 9H), 7.37 (d, $J = 7.9$, 1H), 7.30 (d, $J = 8.7$, 1H), 4.00 (s, 3H), 3.22 (q, $J = 7.2$, 2H), 1.13 (t, $J = 7.2$, 3H). LCMS (ES+, m/z) = 469 $(MH)^+$ (t_R 10.9 min). Anal. ($C_{24}H_{21}ClN_2O_4S$ 0.2 HCO_2H) C, H, N, Cl, S.

***N*-(Cyclopropylmethyl)-4-methoxy-3-({5-[3-(3-pyridinyl)-phenyl]-1,3-oxazol-2-yl}amino)benzenesulfonamide (46).** Following the procedure described for the preparation of isothiocyanate **23**, 3-amino-4-methoxybenzenesulfonyl fluoride was converted to 3-isothiocyanato-4-methoxybenzenesulfonyl fluoride in 94% yield. ^{1}H NMR: δ 8.04 (m, 2H), 7.44 (d, $J =$ 6.4, 1H), 4.01 (s, 3H). Following the general procedure described for the preparation of oxazoles **24**−**33**, 3-bromophenacyl azide and 3-isothiocyanato-4-methoxybenzenesulfonyl fluoride were reacted to produce 3-{[5-(3-bromophenyl)-1,3-oxazol-2-yl]amino}-4-methoxybenzenesulfonyl fluoride in 52% yield. ^{1}H NMR: δ 10.16 (s, 1H), 9.08 (d, $J = 2.4$, 1H), 7.86 (s, 1H), 7.80 (dd, $J = 2.5$, 8.5, 1H), 7.73 (s, 1H), 7.64 (d, $J = 7.6$, 1H), 7.42−7.52 (m, 3H), 4.06 (s, 3H). LCMS (ES+, m/z) = 428 $(MH)^+$. Following the same general procedure for the Stille couplings of oxazole **34**, 3-{[5-(3-bromophenyl)-1,3-oxazol-2-yl]-amino}-4-methoxybenzenesulfonyl fluoride was converted with 3-pyridyltributyltin to 4-methoxy-3-({5-[3-(3-pyridinyl)phenyl]-1,3-oxazol-2-yl}amino)benzenesulfonyl fluoride in 30% yield. ^{1}H NMR: δ 10.05 (s, 1H), 9.02 (d, $J = 2.4$, 1H), 8.90 (d, $J =$ 2.0, 1H), 8.57 (d, $J = 4.5$, 1H), 8.08 (d, $J = 8.1$, 1H), 7.93 (s, 1H), 7.72 (dd, $J = 2.3$, 8.7, 1H), 7.67 (s, 1H), 7.62 (t, $J = 6.9$, 2H), 7.55 (d, $J = 7.7$, 1H), 7.48 (dd, $J = 4.8$, 7.9, 1H), 7.33 (d, $J = 8.8$, 1H), 3.99 (s, 3H). LCMS (ES+, m/z) = 426 $(MH)^+$. 4-Methoxy-3-({5-[3-(3-pyridinyl)phenyl]-1,3-oxazol-2-yl}amino)-benzenesulfonyl fluoride (0.07 g, 0.16 mmol) was dissolved in (cyclopropylmethyl)amine (2 mL) and heated to 100 °C for 16 h in a sealed tube. On cooling, the excess amine was removed on a rotavapor and the crude triturated with methanol to yield the title compound as a white solid (0.04 g, 52%). ^{1}H NMR: δ 9.57 (bs, 1H), 8.91 (s, 1H), 8.67 (d, $J = 1.9$, 1H), 8.57 (d, $J =$ 4.4, 1H), 8.09 (d, $J = 8.1$, 1H), 7.92 (s, 1H), 7.62−7.46 (m, 6H), 7.37 (dd, $J = 1.9$, 7.9, 1H), 7.15 (d, $J = 8.6$, 1H), 3.90 (s, 3H), 2.59 (t, $J = 6.2$, 2H), 0.70−0.81 (m, 1H), 0.29 (t, $J = 7.6$, 2H), 0.03 (d, $J = 5.1$, 2H). LCMS (ES+, m/z) = 477 $(MH)^+$ (t_R 9.7 min).

VEGFR2 HTRF Assay. The assay was performed in 96-well black plates. 10 nM hVEGFR2 was used to phosphorylate 0.36 μM peptide (Biotin-Ahx-EEEEYFELVAKKKK) in the presence of 75 μM ATP, 5 mM $MgCl_2$, 0.3 mM DTT, 0.1 mg/mL BSA, and 0.1 M HEPES (pH 7.5). A 10 μL portion of 0.5 M EDTA was added to reactions as negative controls. The 50 μL kinase reaction with or without inhibitors in 5% DMSO was carried out at room temperature for 45 min and then stopped by 40 μL of 125 mM EDTA. Streptavidin-APC (2.4 μg/mL) and Eu-α-pY (0.15 μg/mL), in the presence of 0.1 mg/mL BSA, 0.1 M HEPES (pH7.5), were added to a final volume of 140 μL. The plate was incubated for 10 min at room temperature and read on the Victor in the time-resolved fluorescence mode by exciting at 340 nm and reading the emission at 665 nm.

Human Umbilical Vein Endothelial Cell (HUVEC) Proliferation Assay (BrdU Incorporation). HUVEC cells and EGM-MV (endothelial cell growth medium−microvascular) were purchased from Clonetics (San Diego, CA). VEGF and bFGF were purchased from R&D Systems (Minneapolis, MN). Anti-BrdU antibody was obtained from Chemicon International (Temecula, CA). HUVECs were routinely maintained in EGM-MV medium and were used within passage 7. HUVECs were plated at a density of 2500 cells/well in M199 medium containing 5% FBS (Hyclone) in a type I collagen-coated plate (Becton Dickinson). The plate was incubated at 37 °C overnight. The medium was removed by aspiration, and test compounds were added to each well in a volume of 0.1 mL/well in serum-free M199 medium. Compound concentrations ranged from 1.5 nM to 30 μM. The plate was incubated for 30 min at 37 °C. Another 0.1 mL of serum-free M199 medium containing BSA and VEGF (or bFGF) was added to give a final concentration of 0.1% BSA and 10 ng/mL VEGF (0.3 ng/mL bFGF). The plate was incubated at 37 °C for 72 h. BrdU was added to each well after the first 48 h to give a concentration of 10 μM. The colorimetric ELISA assay was performed according to manufacturer's (Roche Molecular Sciences) instructions, with detection by absorbance reading at 450 nm. Results were plotted as concentration of test compound vs absorbance to give an IC_{50} value for inhibition of BrdU incorporation.

Pharmacokinetics in Mouse, Rat, and Dog. Oxazole **39** was administered orally to male CD mice ($n = 2$) and male Sprague−Dawley rats ($n = 3$) via oral gavage at a dose volume of 10 mL/kg and by intravenous injection to rats at a dose volume of 5 mL/kg. Oxazole **39** was administered orally to male beagle dogs ($n = 2$) via oral gavage and by intravenous injection at a dose volume of 0.5 mL/kg. The blood samples were placed on wet ice, and plasma was collected after centrifugation. Plasma samples were stored frozen at −20 °C until time of analysis. Plasma samples were prepared by protein precipitation with four volumes of acetonitrile (200 μL) per 50 μL of plasma sample. Samples were analyzed by high-performance liquid chromatography (HPLC)/mass spectrometric analysis. Pharmacokinetic parameters were determined by PKCal 2.0.

Antitumor Activity against HT29 Colon Carcinoma Xenograft Model. HT29 tumors were initiated by injection of tumor cell suspension subcutaneously in 8−12 week old female nude mice. Mice were randomized into groups of eight prior to treatment when tumors reached a volume of 50−60 mm^3 (9 days after implantation). Animals were treated with oxazole **39** (30 or 100 mg/kg) or vehicle (in 0.5% HPMC, 0.1% Tween 80 in sterile water), administered once daily by oral gavage. Tumor volume was measured twice weekly by calipers, using the formula (length × width^2 × 0.5), where length was the longest diameter across the tumor, and width was the corresponding perpendicular. Tumor growth inhibition was calculated by mean change in tumor volume of control and treated groups. All animal studies were performed under approved protocols from the institutional animal care and use committee.

Crystallography of VEGFR2 Ligand Complexes. Protein expression and purification of human VEGFR2 was carried out as described by McTigue et al.[21,22] Protein−ligand complexes were obtained by combining 100 μL of the protein solution (VEGFR: 10 mg/mL, 10 mM Hepes, pH 7.5, 10 mM DTT, and 10 mM NaCl) with 3 μL of a 50 mM compound in DMSO and allowing the mixture to stand for 90 min at 20 °C. Crystals of the complex were obtained using the hanging drop method using drops composed of 1:1 of the protein/ligand complex and 4 μL of a reservoir solution (100 mM Hepes, pH 7.5, 2.1 M ammonium sulfate, and 2% PEG550). X-ray data was collected from cryogenically preserved crystals using a Mar165 detector at Sector 17 of the Advanced Photon Source. Crystal structures were solved using the Amore molecular replacement program[23] with an unligand structure of VEGFR2 as the search model. The structures were built using the program O,[24] and initial refinement was carried out with the CNX program.[25] Map generation, density modification, and final refinement was carried out using programs from the CCP4 Suite.[23]

Acknowledgment. We acknowledge Sue Kadwell and Earnest Horne for generating the construct and expression vectors used for protein production and Warren Rocque and William Holmes for the production of protein. X-ray data was collected at beam line 17-ID in the facilities of the Industrial Macromolecular Crys-

tallography Association Collaborative Access Team (IMCA-CAT) at the Advanced Photon Source. Use of the Advanced Photon Source was supported by the U. S. Departmentof Energy, Basic Energy Sciences, Office of Science, under Contract No. W-31-109-Eng-38. We are grateful to Peter Kitrinos and Amanda G. Alford for MS and HPLC support, respectively.

Supporting Information Available: Elemental analysis, HRMS, LCMS, and HPLC data for **5**, **8**−**46**. This material is available free of charge via the Internet at http://pubs.acs.org.

References

(1) Folkman, J. Fundamental Concepts of the Angiogenic Process. *Curr. Mol. Med.* **2003**, *3*, 643−651.
(2) Veikkola, T.; Karkkainen, M.; Claesson-Welsh, L.; Alitalo, K. Regulation of Angiogenesis via Vascular Endothelial Growth Factor Receptors. *Cancer Res.* **2000**, *60*, 203-212.
(3) Glade-Bender, J.; Kandel, J. J.; Yamashiro, D. J. VEGF Blocking Therapy in the Treatment of Cancer. *Expert Opin. Biol. Ther.* **2003**, *3*, 263−276.
(4) Hurwitz, H.; Fehrenbacher, L.; Novotny, W.; Cartwright, T.; Hainsworth, J.; Heim, W.; Berlin, J.; Baron, A.; Griffing, S.; Holmgren, E.; Ferrara, N.; Fyfe, G.; Rogers, B.; Ross, R.; Kabbinavar, F.; Bevacizumab plus irinotecan, fluorouracil, and leucovorin for metastatic colorectal cancer. *N. Engl. J. Med.* **2004**, 350, 2335−2342.
(5) Lu, D.; Jimenez, X.; Zhang, H.; Bohlen, P.; Witte, L.; Zhu, Z. Selection of high affinity human neutralizing antibodies to VEGFR2 from a large antibody phage display library for antiangiogenesis therapy *Int. J. Cancer* **2002**, *97*, 393−399.
(6) Holash, J.; Davis, S.; Papadopoulos, N.; Croll, S. D.; Ho, L.; Russell, M.; Boland, P.; Leidich, R.; Hylton, D.; Burova, E.; Ioffe, E.; Huang, T.; Radziejewski, C.; Bailey, K.; Fandl, J. P.; Daly, T.; Wiegand, S. J.; Yancopoulos, G. D.; Rudge, J. S. VEGF-Trap: A VEGF blocker with potent antitumor effects. *Proc. Natl. Acad. Sci. U.S.A.* **2002**, *99*, 11393−11398.
(7) Bold, G.; Altman, K.-H.; Frei, J.; Lang, M.; Manley, P. W.; Traxler, P.; Weitfeld, B.; Bruggen, J.; Buschdunger, E.; Cozens, R.; Ferrari, S.; Furet, P.; Hofmann, F.; Martiny-Baron, G.; Mestan, J.; Rosel, J.; Sills, M.; Stover, D.; Acemoglu, F.; Boss, E.; Emmenegger, R.; Lasser, L.; Masso, E.; Roth, R.; Schlachter, C.; Vetterli, W.; Wyxx, D.; Wood, J. M. New anilinophthalazines as potent and orally well absorbed inhibitors of the VEGF receptor tyrosine kinase useful as antagonists of tumor-driven angiogenesis. *J. Med. Chem.* **2000**, *43*, 2310−2323.
(8) Hennequin, L. F.; Stokes, E. S.; Thomas, A, P.; Johnstone, C.; Ple, P. A.; Ogilvie, D. J.; Dukes, M.; Wedge, S. R.; Kendrew, J.; Curwen, J. O. Novel 4-anilinoquinazolines with C-7 basic side chains: Design and structure activity relationship of a series of potent, orally active, VEGF receptor tyrosine kinase inhibitors. *J. Med. Chem.* **2002**, *45*, 1300−1312.
(9) Mendel, D. B.; Laird, A. D.; Xin, X.; Louie, S. G.; Christensen, J. G.; Li, G.; Schreck, R. E.; Abrams, T. J.; Ngai, T. J.; Lee, L. B.; Murray, L. J.; Carver, J.; Chan, E.; Moss, K. G.; Haznedar, J. O.; Sukbuntherng, J.; Blake, R. A.; Sun, L.; Tang, C.; Miller, T.; Shirazian, S.; McMahon, G.; Cherrington, J. M. In Vivo Antitumor Activity of SU11248, a Novel Tyrosine Kinase Inhibitor Targeting Vascular Endothelial Growth Factor and Platelet-derived Growth Factor Receptors: Determination of a Pharmacokinetic/Pharmacodynamic Relationship. *Clin. Cancer Res.* **2003**, *9*, 327−337.
(10) Beebe, J. S.; Jani, J. P.; Knauth, E.; Goodwin, P.; Higdon, C.; E.; Rossi, A. M.; Emerson, E.; Finkelstein, M.; Floyd, E.; Harriman, S.; Atherton, J.; Hillerman, S.; Soderstrom, C.; Kou, K.; Grant, T.; Noe, M. C.; Foster, B.; Rastinejad, F.; Marx, M. A.; Schaeffer, T.; Whalen, P. M.; Roberts, W. G. Pharmacological Characterization of CP-547,632, a novel vascular endothelial growth factor receptor-2 tyrosine kinase inhibitor for cancer therapy. *Cancer Res.* **2003**, *63*, 7301−7309.
(11) Brown, M. L.; Cheung, M.; Dickerson, S. H.; Gauthier, C.; Harris, P. A.; Hunter, R., N.; Pacofsky, G.; Peel, M. R.; Stafford, J. A. Chemical Compounds. *PCT Int. Appl.,* **2004**, WO 2004032882.
(12) Sych, E. D.; Belaya, Zh. N.; Moreiko, O. V. Synthesis of azole derivatives. IV. Reaction of aminomethyl and (alkylamino)-methyl ketones with carbon disulfide. *Khim. Geterotsikl. Soedin.* **1970**, No. 2 282-285. (*Chem. Abstr. 76*: 140606).
(13) Harrison, R. G. Oxazole derivatives. Ger. Offen. 1976, 2,459,-380 (*Chem. Abstr. 86*: 121320).
(14) Froeyen, P. New applications of iminophosphoranes. The preparation of β-keto carbodiimides and their rearrangement to 2-amino-1,3-oxazoles. *Phosphorus, Sulfur Silicon Relat. Elements* **1991**, *60*, 81−84.
(15) Mohammadi M.; Froum S.; Hamby J. M.; Schroeder M. C.; Panek R. L.; Lu G. H.; Eliseenkova A. V.; Green D.; Schlessinger J.; Hubbard S. R. Crystal structure of an angiogenesis inhibitor bound to the FGF receptor tyrosine kinase domain. *EMBO J.* **1998**, *17,* 5896−5904.
(16) Mohammadi M.; McMahon G.; Sun L.; Tang C.; Hirth P.; Yeh B. K.; Hubbard S. R.; Schlessinger J. Structures of the tyrosine kinase domain of fibroblast growth factor receptor in complex with inhibitors. *Science* **1997**, *276*, 955−960.
(17) Nagar, B.; Bornmann, W. G.; Pellicena, P.; Schindler, T.; Veach, D. R.; Miller, W. T.; Clarkson, B.; Kuriyan, J. Crystal Structure of the Kinase Domain of c-Abl in Complex With the Small Molecule Inhibitors PD173955 and Imatinib (STI-571). *Cancer Res*. **2002**, *62*, 4236−4243.
(18) Schindler T.; Sicheri F.; Pico A.; Gazit A.; Levitzki A.; Kuriyan J. Crystal structure of Hck in complex with a Src family-selective tyrosine kinase inhibitor. *Mol. Cel.,* **1999**, *3*, 639−648.
(19) Zhu X.; Kim J. L.; Newcomb J. R.; Rose P. E.; Stover D. R.; Toledo L. M.; Zhao H.; Morgenstern K. A. Structural analysis of the lymphocyte-specific kinase Lck in complex with non-selective and Src family selective kinase inhibitors. *Structure Fold Des*. **1999**, *7*, 651−661.
(20) Stamos J.; Sliwkowski M. X.; Eigenbrot C. Structure of the epidermal growth factor receptor kinase domain alone and in complex with a 4-anilinoquinazoline inhibitor. *J. Biol. Chem*. **2002**, *277*, 46265−46272.
(21) McTigue, M. A.; Wickersham, J. A.; Pinko, C.; Showalter, R. E.; Parast, C. V.; Tempczyk-Russell, A. Gehring, M. R.; Mroczkowski, B. Kan, C.-C.; Vllafranca, J. E. Appelt, K. Crystal Structure of the Kinase Domain of Human Vascular Endothelial Growth Factor Receptor 2: A Key Enzyme in Angiogenesis. *Structure* **1999**, *7*, 319−330.
(22) Coordinates may be obtained from the RCSB Protein data bank under accession codes 1Y6A (oxazole **39**) and 1Y6B (oxazole **46**).
(23) Collaborative Computational Project, Number 4, The *CCP*4 suite: Programs for protein crystallography. *Acta Crystallogr.* **1994**, *D50*, 760−763.
(24) Jones, T. A.; Bergdoll, M.; Kjeldgaard, M. O: A macromolecule modeling environment. *Crystallogr. Model. Methods Mol. Des., [Pap. Symp.]* Bugg, C. E., Ed.; Springer: New York, 1990; pp 189−199.
(25) Brunger, A. T.; Adams, P. D.; Clore, G. M.; DeLano, W. L.; Gros, P.; Grosse-Kunstleve, R. W.; Jiang, J.-S.; Kuszewski, J.; Nilges, M.; Pannu, N. S.; Read, R. J.; Rice, L. M.; Simonson, T.; Warren, G. L. Crystallography & NMR system: A new software suite for macromolecular structure determination. *Acta Crystallogr., Sect. D: Biol. Crystallogr.* **1998**, *D54*, 905−921.

JM049538W